Supplementary Material

# Acid-reagent-engineered tunable multicolor carbon dots via solid-phase pyrolysis for advanced information encryption and anti-counterfeiting

Jin Chai,[a] Caiqin Su,[a] Yide Han,[a] Wenhao Li,[a] Nan Wang,[b] Wengao Zhang,[c] Xia Zhang*[a]

[a] J. Chai, Y. Han, W. Li, X. Zhang
Department of Chemistry, College of Sciences
Northeastern University
No.3-11 Wenhua Road, Heping District, Shenyang, 110819, P. R. China
E-mail: xzhang@mail.neu.edu.cn
[b] N. Wang
Analytical and Testing Center
Northeastern University
No.3-11 Wenhua Road, Heping District, Shenyang, 110819, P. R. China
E-mail: wangnan001050@163.com
[c] W. Zhang
School of Materials Science and Engineering
Southern University of Science and Technology
No. 1088 Xueyuan Boulevard, Nanshan District, Shenzhen, 518055, P. R. China
E-mail: 1435669101@qq.com

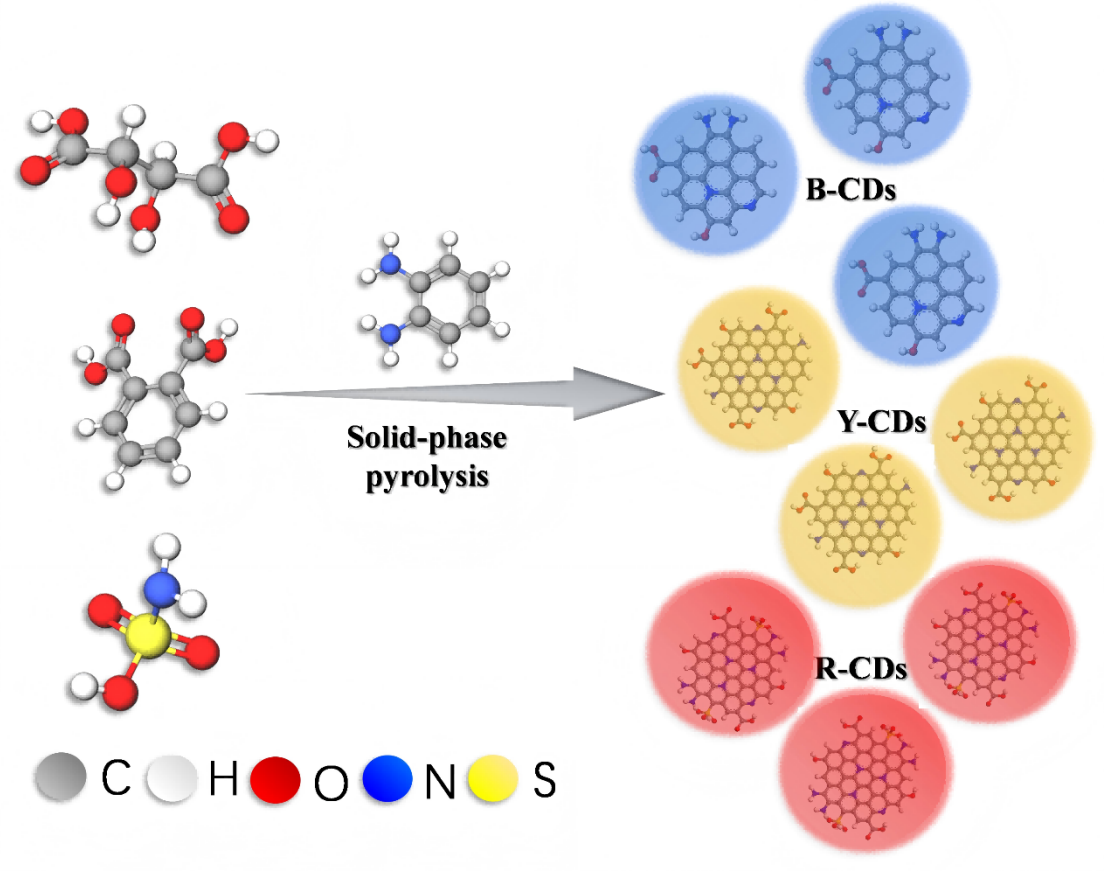


Fig. S1 Illustration of the synthesis of three CDs.

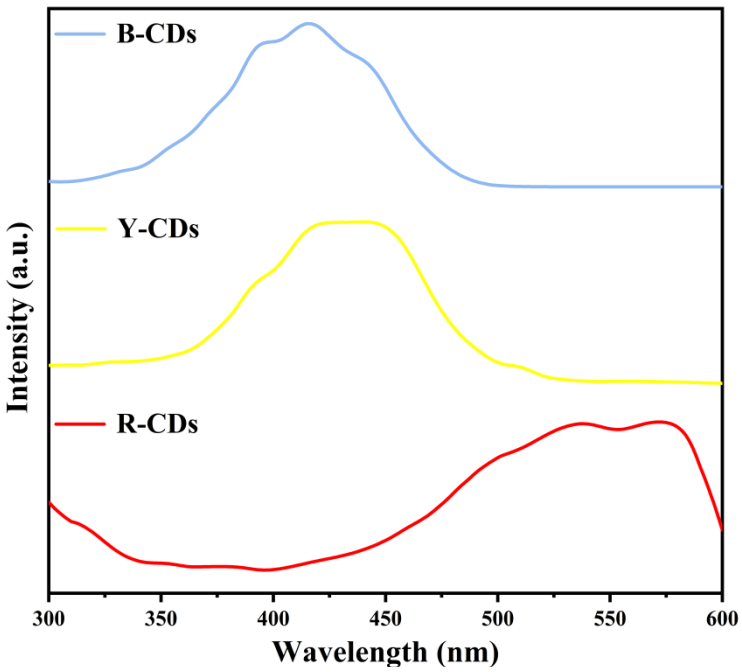


Fig. S2 PL excitation spectra of B-CDs, Y-CDs, and R-CDs.

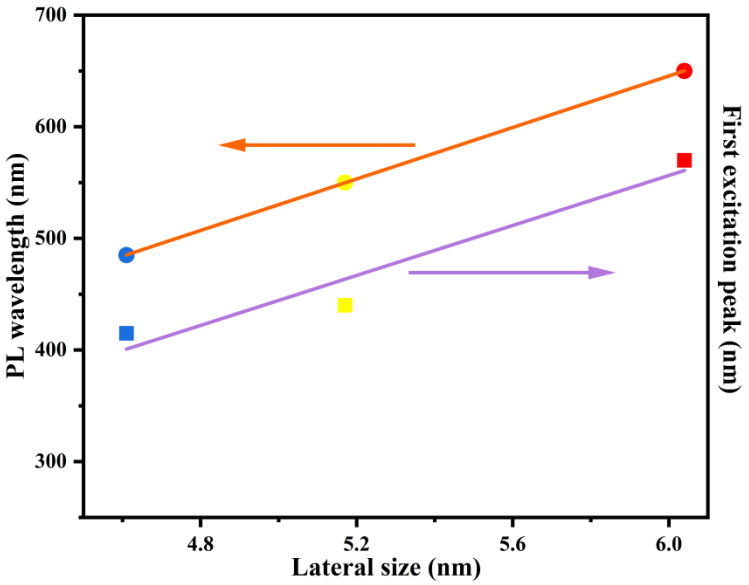


Fig. S3 Dependence of the PL wavelength and first excitonic absorption band on the particle size of CDs.

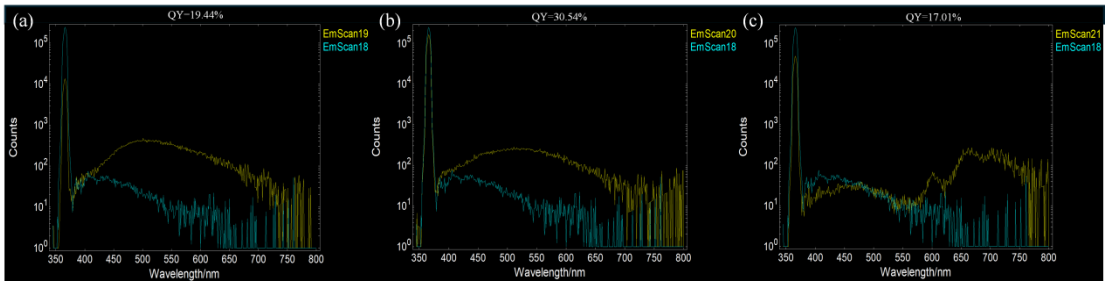


Fig. S4 The photoluminescence quantum efficiency of B-CDs (a), Y-CDs (b), and R-CDs (c).

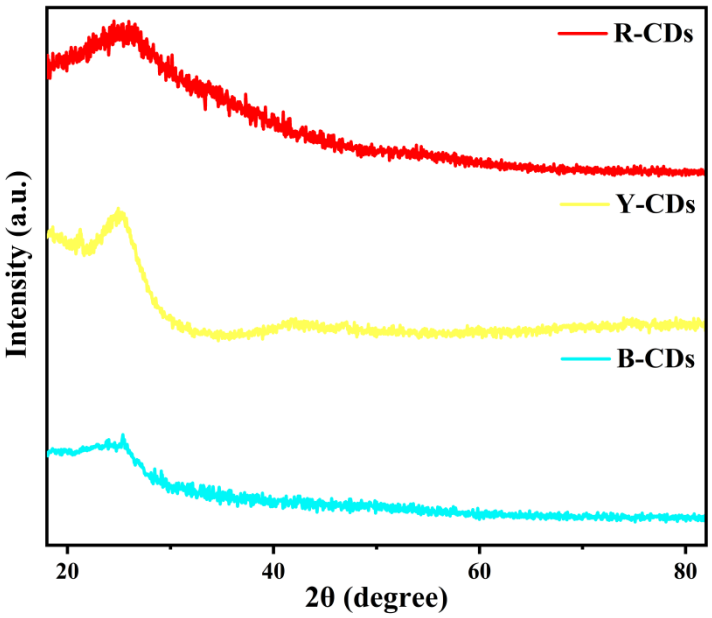


Fig. S5 The XRD patterns of B-CDs, Y-CDs and R-CDs.

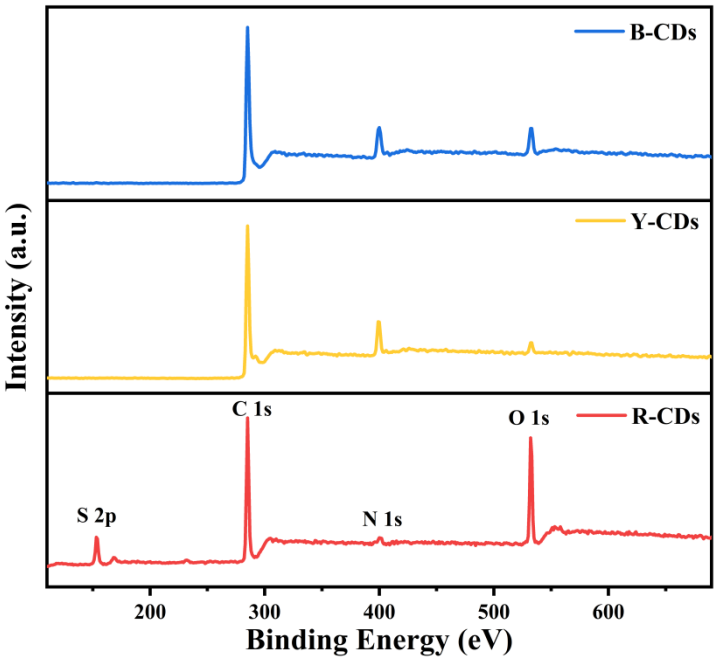


Fig. S6 Full-survey X-ray photoelectron spectroscopy (XPS) spectra of B-CDs, Y-CDs and R-CDs.

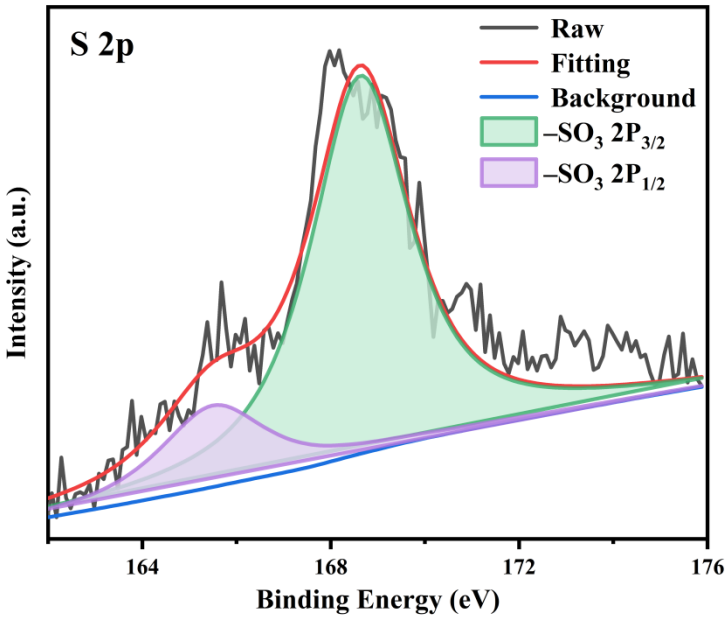


Fig. S7 High-resolution XPS spectra of S 2P of R-CDs.

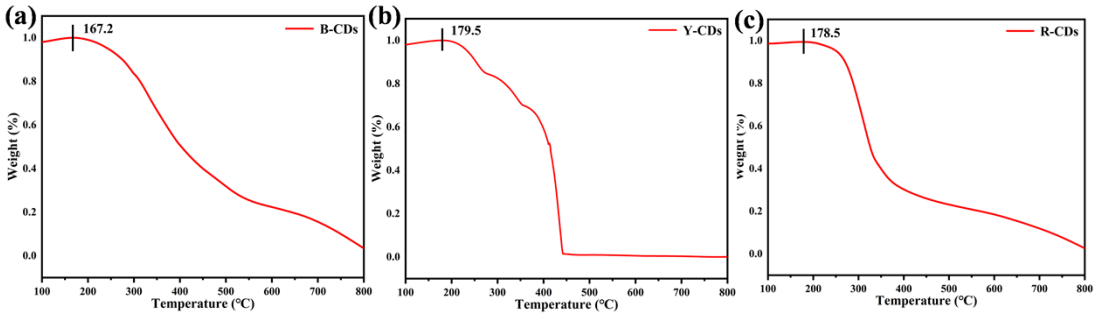


Fig. S8 Thermogravimetric analysis (TGA) of B-CDs, Y-CDs, and R-CDs.

## Table

Table S1 Table of fitting parameters for fluorescence lifetime of three CDs.

| Sample | $\tau_1$ (ns) | $B_1$ | $\tau_2$ (ns) | $B_2$ | $\tau_{int}$ (ns) |
|---|---|---|---|---|---|
| B-CDs | 2.70 | 312.42 | 8.55 | 244.24 | 6.87 |
| Y-CDs | 0.84 | 602.57 | 6.11 | 75.73 | 3.35 |
| R-CDs | 1.41 | 560.89 | 4.03 | 52.84 | 1.97 |

Table S2 Contents of C–C/C=C, C–N/C–O, and C=O bonds in the three CDs.

| Sample | C–C/C=C | C–N/C–O | C=O |
|---|---|---|---|
| B-CDs | 44.54% | 44.81% | 10.65% |
| Y-CDs | 46.94% | 41.94% | 11.12% |
| R-CDs | 50.99% | 42.14% | 6.87% |

Table S3 Contents of Pyridinic N, Pyrrolic N, Graphitic N, and Amino N in the three CDs.

| Sample | Pyridinie N | Pyrrolie N | Graphitie N | Amino N |
|---|---|---|---|---|
| B-CDs | 24.40% | 24.87% | 19.18% | 31.53% |
| Y-CDs | 23.48% | 24.30% | 30.58% | 21.64% |
| R-CDs | 15.53% | 25.41% | 39.16% | 19.90% |

Table S4 Contents of C–O, C=O, and S–O/S=O bonds in the three CDs.

| Sample | C–O | C=O | S–O/S=O |
|---|---|---|---|
| B-CDs | 64.07% | 35.93% | —— |
| Y-CDs | 59.83% | 40.17% | —— |
| R-CDs | 47.99% | 30.98% | 21.03% |

Table S5 The HOMO-LUMO energy levels, the energy gap (ΔE), and the corresponding predicted emission wavelength (based on the ΔE).

| Mode | HOMO | LUMO | ΔE | λ (nm) |
|---|---|---|---|---|
| A | -4.96 | -2.33 | 2.64 | 470.58 |
| B | -4.68 | -2.76 | 1.92 | 644.72 |
| C | -4.67 | -2.65 | 2.02 | 613.70 |
| D | -4.65 | -2.64 | 2.01 | 615.52 |
| E | -5.10 | -3.43 | 1.68 | 739.52 |